

# Validation of Large Eddy Simulation in a Relaminarizing Boundary Layer Flow

Jianbo Jiang<sup>1c</sup> and Xinlei Wang<sup>2</sup>

<sup>1</sup> Monell Chemical Senses Center, Philadelphia, PA 19104 USA

<sup>2</sup> Department of Agricultural and Biological Engineering, University of Illinois, Urbana, IL 61801 USA

Received: 18/04/2011 – Revised 30/07/2011 – Accepted 24/10/2011

## Abstract

Coexistence of laminar, transitional and turbulent flow regimes is very common in blood flows through arteries, airflows in human respiratory systems, and indoor airflow etc. Due to the complexity of flow physics involved, most Reynolds-averaged Navier-Stokes (RANS) turbulence models are not suitable for these flows because they are designed primarily for high Reynolds number turbulent flows. In this paper, large eddy simulation with dynamic subgrid scale model has been applied to simulate the flow in a relaminarizing boundary layer that undergoes reverse transition from turbulent state to laminar one. Simulated mean velocities and turbulent intensities are in good agreement with corresponding experimental data at different streamwise positions where different flow regimes exist. The appropriateness of dynamic subgrid scale model for the study of relaminarizing boundary layer flow is demonstrated by the variation of subgrid constant: it is somewhat constant in fully turbulent regime, decreases in transitional regime and reaches zero in laminar regime. Comparison of the experimental data and computational results from three low Reynolds number RANS models shows that they do not adequately predict the flow relaminarization. The present study suggests the use of large eddy simulation with dynamic model in the study of complex flows where a combination of flow regimes (laminar, transitional, and turbulent) may exist.

*Keywords: Large Eddy Simulation; Dynamic subgrid scale model; Relaminarizing boundary layer; RANS models; Transitional flow.*

## 1. Introduction

Flows in the arteries, respiratory systems and cardiovascular systems are generally laminar due to the low Reynolds number. However, in the presence of local area reductions, these flows could become turbulent via a transitional region [1]. On the other hand, the originally turbulent flows in airway bifurcation could be relaminarized into laminar flows due to the effects of branching on flow rates [7, 22]. The coexistence of laminar, transitional, and turbulent regimes is also very common in indoor enclosure [36], high-lift systems [5] and paper making machinery [23].

<sup>c</sup> Corresponding Author: Jianbo. Jiang

Email: [bjjiang@gmail.com](mailto:bjjiang@gmail.com)

Telephone: +267 5194937

Fax: +267 5194937

© 2009-2012 All rights reserved. ISSR Journals

PII: S2180-1363(12)4111-X

Accurate prediction of such complex flows is very challenging. Most of the commonly used Reynolds Averaged Navier-Stokes (RANS) models are not appropriate for such flows due to their underlying assumption that flows are fully turbulent. Several previous studies [10, 26, 33, 35] have shown that predictions of these flows based on RANS turbulence models are unsatisfactory even when advanced turbulence models such as Reynolds Stress transport models are used. While direct numerical simulation (DNS) is a very accurate numerical method and could be used to prediction of such flows [4, 19, 29] at low Reynolds number, application of DNS would be extremely expensive and not applicable for high Reynolds number flow because the number of grid points needed is prohibitively large in order to accurately resolve all the spatial and temporal scales [21].

Large eddy simulation (LES) is a promising approach to predict the flows where laminar, transitional and turbulent regimes are all present. LES could be considered to lie between RANS and DNS: only large scales are resolved while small ones are modelled [25, 30]. Advantages of LES over RANS and DNS include substantial lower resolution requirements than DNS and more accurate than RANS. Luo et al [18] and Beech-Brandt et al [3] have used LES with the Smagorinsky subgrid model to investigate the flows in a tube with an axsymmetric stenosis where both laminar and transitional/turbulent flow coexisted [27]. However, the improvement over RANS models [9, 31] is only modest. This is possibly due to the inherent limitation of the Smagorinsky subgrid model where a fixed value of Smagorinsky constant is adopted. It has been found that the Smagorinsky constant is not universal and several commonly used non-zero values can cause excessive damping of large-scale fluctuations in the presence of mean shear and in transitional flows as near solid boundary [8]. The dynamic model for subgrid-scale (SGS) developed by Germano et al [8] is a major advance in the development of LES models for predicting the transitional and turbulent channel flows. In this model, the Smagorinsky constant is not specified a priori, but dynamically calculated based on the information from the resolved large scales. It varies both spatially and temporally, more importantly, reduces its value in transitional flows and becomes zero in laminar flows [8]. Mittal et al [19, 20] applied this model to study the pulsative flows in a constricted channel over a range of Reynolds numbers and found that flows underwent transitions from laminar flows to turbulence for Reynolds number higher than 1000. However, no corresponding validation experiments existed for their simulations thus only flow behavior similarities were noted against related experiments [11, 15].

The goal of the present paper is to validate LES with dynamic subgrid scale model for the predictions of complex flow where turbulent, transitional and laminar flows coexist. A relaminarization boundary layer flow [32] is selected as the test case. Besides the coexistence of different flow regimes in this flow, it has several desirable features for validating purpose such as relatively simple geometry, well-defined inflow conditions and existence of analytic solution in laminar regime. As the flow characteristics near the walls play an important role in the genesis and acceleration of diseases in cardiovascular system [19], the present paper is mainly focused on the capability of dynamic LES in the predictions of near wall flow behaviours.

## 1. Numerical details

The governing equations for LES are obtained by applying a spatial filter to the Navier-Stokes equations:

$$\frac{\partial \bar{u}_i}{\partial x_i} = 0 \quad (1)$$

$$\frac{\partial \bar{u}_i}{\partial t} + \frac{\partial \bar{u}_i \bar{u}_j}{\partial x_j} = -\frac{\partial \bar{P}}{\partial x_i} + \frac{1}{\text{Re}} \frac{\partial^2 \bar{u}_i}{\partial x_j \partial x_j} - \frac{\partial \tau_{ij}}{\partial x_i} \quad (2)$$

where  $Re$  is Reynolds number and  $\bar{Q}(\mathbf{x}, t) = \int_{-\infty}^{+\infty} Q(\mathbf{x}, t) G(\mathbf{x} - \mathbf{x}') d\mathbf{x}'$ ,  $Q$  is velocity ( $u$ ) or pressure ( $P$ ) and  $G$  is the filter.  $\tau_{ij}$  is the sub-grid stress (SGS) and needs to be modeled.

The Smagorinsky subgrid model [30] takes the following form:

$$\tau_{ij} = -2\nu_t \bar{S}_{ij} + \frac{1}{3} \tau_{ii} \delta_{ij} \quad (3)$$

where  $\nu_t = \bar{L}^2 |\bar{S}|$ ,  $|\bar{S}| = \sqrt{2\bar{S}_{ij}\bar{S}_{ij}}$ ,  $\bar{S}_{ij} = \frac{1}{2} \left( \frac{\partial u_i}{\partial x_j} + \frac{\partial u_j}{\partial x_i} \right)$  and  $\bar{L} = C_s V^{1/3}$ ,  $V$  is the volume of the cell. The commonly used value of  $C_s$  is 0.1. The dynamic subgrid scale model ([8, 17]) used in this study computed  $C_s$  in a dynamical procedure based on the information from the resolved large scales of motion. More details about the implementation of this model can be found in Germano et al [8], Lilly [17], and Kim et al [37].

The computational domain adopted in present study is shown in Figure 1. The boundaries consist of inflow and outflow boundaries, located at  $x = -430$  mm and  $x = 1430$  mm respectively, and solid boundaries in the other regions. Mean (bulk) velocity at the inlet is 3m/s and corresponding Reynolds number (based on bulk velocity and inlet height) is equal to 50000. In order to eliminate the uncertainties related to the inlet conditions, a separate duct flow simulation was carried out to provide the inflow conditions. A convective outflow condition was applied at the outlet. Uniform grids were used in the streamwise direction while non-uniform grids were used in vertical and spanwise directions. The grids near the wall were very dense: at least 10 cells were put within the viscosity-affected near wall region and the wall unit values ( $y^+ = u_\tau y_p / \nu$ , where  $u_\tau$  is the wall friction velocity,  $y_p$  is distance from first grid point to the wall, and  $\nu$  is kinematic viscosity of the fluid) were less than 1. Grid independence was studied through two sets of mesh,  $120 \times 96 \times 80$  and  $176 \times 159 \times 120$ . There is no much difference (less than 2.5%) in the results between the two meshes in terms of mean velocity and turbulent intensity.

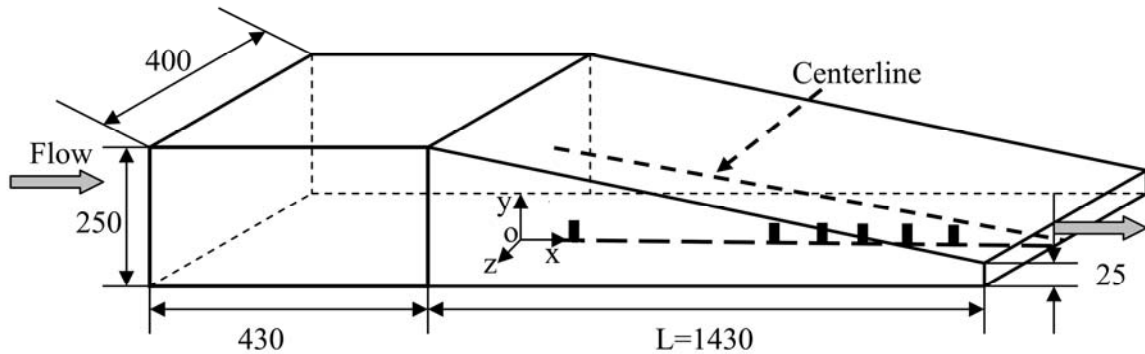


Figure 1. Schematic of computational domain (all units are mm), where centerline connects the centers of two contraction planes.  $x$ ,  $y$ , and  $z$  represent the streamwise, vertical and spanwise directions. Shaded rectangles represent (from left to right) the streamwise positions of  $x/L=0.04$ ,  $0.51$ ,  $0.62$ ,  $0.69$ , and  $0.83$  respectively, where  $L$  is the length of the converging channel

All the computations were performed using the commercial computational fluid dynamics software package FLUENT 6.3. A bounded, second-order-accurate central differencing scheme was used for the spatial discretization and the non-iterative time-advancement/fractional-step scheme was used for the temporal discretization. After several characteristic time units (one time unit  $T$  could be calculated by the ratio of domain length to mean inlet velocity), the flows reached statistically steady state. From then, flow statistics were gathered over about  $12T$ .

## 2. Results and discussion

### 2.1. Experimental data

The numerical results were compared with detailed experimentally measured velocity and turbulent intensity profiles from Talamelli et al [32]. The computational domain shown in Figure 1 corresponds exactly to the upper half of the experimental set-up while the bottom wall ( $y=0$ ) of the computational domain corresponds to the aluminium flat plate mounted at the symmetry plane of a two-dimensional convergent channel. The inlet velocity is about 3 m/s and air is accelerated in the two dimensional contraction after it leaves the rectangular duct due to the strong favorable pressure gradient. Axial velocities and turbulent intensities at different streamwise positions (see Figure 1) were measured with constant temperature single probe hotwire anemometers. The initially turbulent boundary layer on the bottom wall gradually turned into the laminar flow, which was confirmed by the variation of mean velocity and turbulent intensity profiles along the streamwise positions (Figure2).

### 2.2. Comparison of mean velocities and turbulent intensities

Figure 2(a) shows the comparison of calculated mean velocities with measurements at five streamwise positions. Self-similar laminar solution of the boundary layer equations in a contracting channel [28] is also included. The solution is obtained by introducing the similarity transformation (4) into the two-dimensional boundary layer governing equations,

$$\eta = y\sqrt{U_e/\nu(x_0 - x)} \quad (4)$$

where  $U_e$  is the mean local free stream velocity and  $x_0$  is the virtual point of contraction. The governing equations using the stream function formulation are thus transformed into a third-order ordinary differential equation, which can be solved analytically for known boundary conditions. The analytical solution is written as,

$$u(\eta)/U_e = 3 \tanh^2\left(\eta/\sqrt{2} + 1.146\right) - 2 \quad (5)$$

More details about the solution procedures can be found in [28].

At the beginning of the contraction ( $x/L=0.04$ , where  $L$  is the length of the contraction channel, see Figure 1), mean velocity profiles of a turbulent boundary layer were observed in the experiments. At the downstream streamwise locations ( $x/L=0.51$ ,  $0.62$ , and  $0.69$ ), the viscous boundary sublayer thickness increased and transition from a turbulent to laminar state began. The characteristics of transitional boundary flow in the above three locations were demonstrated by the velocity profiles and confirmed by the profiles of three boundary layer thickness parameters (displacement thickness, the momentum loss thickness and the shape factor) [32]. At the further downstream  $x/L=0.83$ , full relaminarization was observed measured mean velocities agreed well with the self-similar laminar solution. As can be seen in Figure 2(a), LES calculations agree excellently with experimental data at the five streamwise positions investigated. A comparison (data not shown) of free stream mean velocities  $U_e$  was also made between simulation, measurement, and analytic inviscid solution ( $U_e/U_0 = 1 - x/L$ , where  $U_0$  is the velocity at the channel inlet) for the flow through the channel [32]. The simulated streamwise velocities at the centerline of the contraction channel (see Figure 1) were adopted for comparison and the good agreement was found between simulated results, experimental data and analytic solution, indicating an accurate prediction of free stream velocity at each streamwise position.

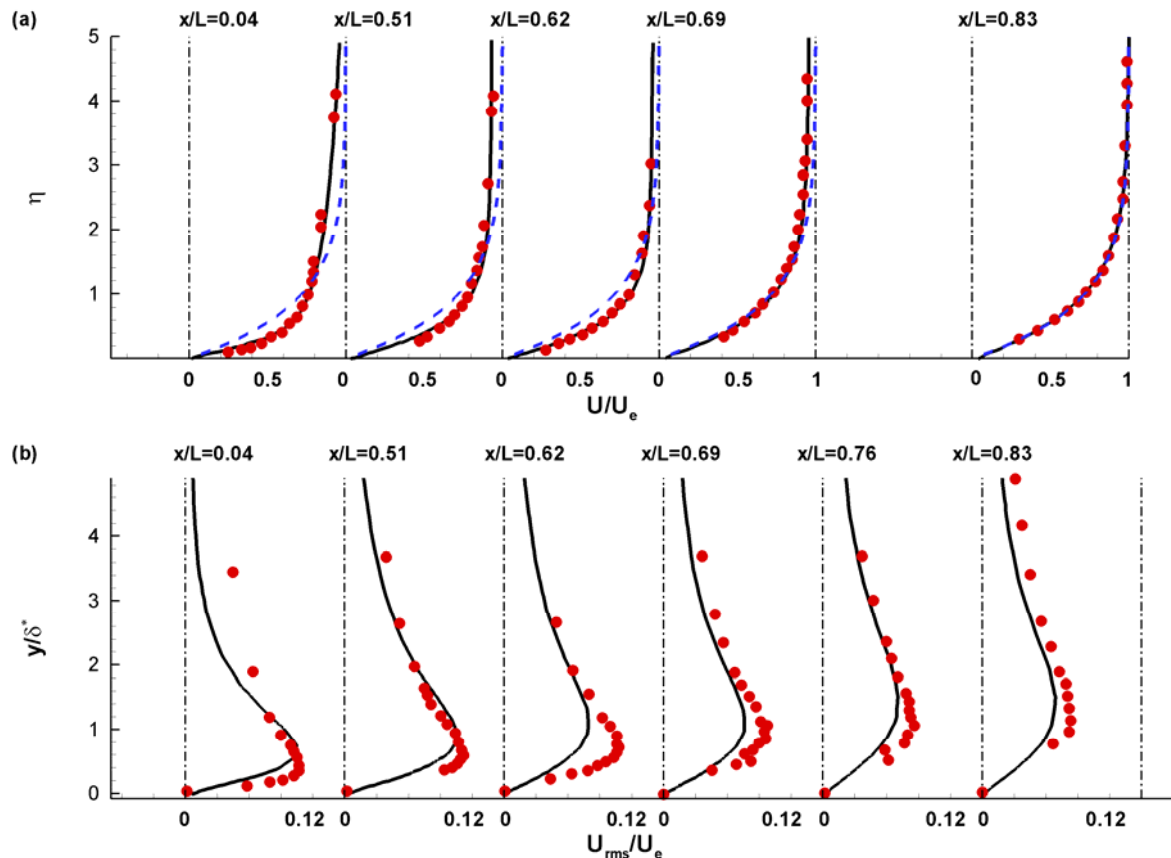


Figure 2. (a) Comparison of mean velocities between simulation and experiments; (b) Comparison of turbulent fluctuations between simulation and experiments. LES, EXP, and ANA represent the results from LES simulation, experiment, and analytical laminar solution

The process of relaminarization is also characterized by the decrease of turbulent intensity and shift away of the position of its maximum value from the wall [32]. Figure 2 (b) shows the comparison of calculated turbulent intensities with measurements at the five different streamwise positions and one additional position ( $x/L=0.76$ ). The overall agreement is fairly good except that LES results are on a lower level than measurements in all the six positions. It is hard to pinpoint the exact reason for the relative disagreement between simulation and experimental data. LES calculation with dynamic kinetic energy model [12] was conducted to check the effects of subgrid model. Unfortunately, we found the later model generated similar results as dynamic subgrid scale model and relatively lower values of turbulent intensities were still predicted when compared to experimental data. One more possible reason is that the central differencing scheme for spatial discretization implemented in Fluent is still slightly dissipative and the resolved turbulent fluctuations were possibly damped out in part by numerical dissipation. Further analysis of this issue is needed and left for future work.

However, it is important to note that the LES with dynamic model still somehow captured the characteristics of relaminarization process. In consistence with experimental data, predicted turbulence intensities in the five streamwise positions decreased with increase of distance from the start of the contraction. Furthermore, the move away of the position of maximum turbulent intensities from the wall was also reflected in the simulation results in the downstream.

### 2.3. Spatial variation of subgrid constant $C_s$

Figure 3 shows streamwise variation of subgrid constant  $C_s$ , averaged both in the vertical direction (y-direction, see Figure 1), spanwise direction (z-direction, see Figure 1) and time. The relaminarization process is clear reflected through the spatial variations of  $C_s$ : it remains relatively constant (about 0.125) in fully turbulent boundary layer ( $x/L < 0.1$ ), decreases in transitional flows ( $0.1 < x/L < 0.7$ ), and approaches zero in laminar boundary layer ( $x/L > 0.7$ ). Thus the subgrid constant could be chosen as a parameter for detection of occurrence of turbulent boundary layer relaminarization. Figure 3 also implies that the standard Smagorinsky subgrid model would have difficulties in the prediction of relaminarizing boundary flow since an ad hoc constant  $C_s$  is needed.

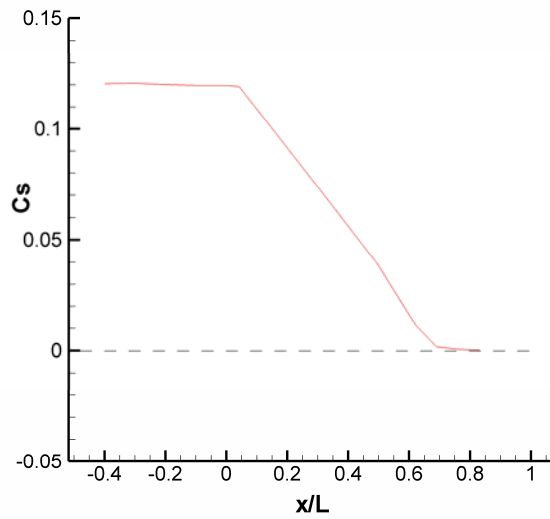


Figure 3. Streamwise variation of averaged subgrid constant

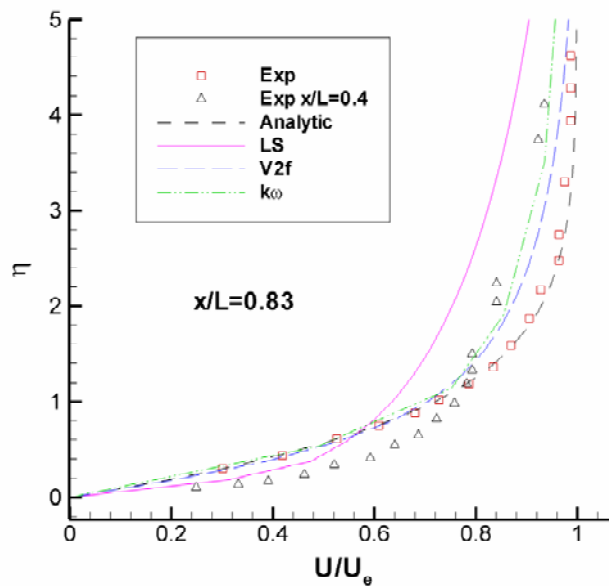


Figure 4. Comparison of mean velocities between experiments and RANS models at  $x/L=0.83$  in the laminar regime. Square: measured data; Dashed: analytic solution; Solid: LS model prediction; Long dashed: V2f model prediction; Dashed dot dot:  $k-\omega$  model prediction. Measured data at  $x/L=0.04$  (Delta) in turbulent regime were included for comparison

## 2.4. Evaluation of RANS models

Some attempts to compute this flow with traditional RANS models have also been conducted. Figure 4 shows the comparison between measured velocities and predictions with three RANS models in the laminar boundary layer region ( $x/L=0.83$ ). Patel et al [24], Aupoix and Viala [2] studies show, among several low Reynolds turbulence models, LS model [13] and  $k-\omega$  model [34] performed considerably better than the other models in the predicting relaminarization. In addition, Lien et al [16] demonstrated the capability of V2f model [6] in the capture of transitional effects. In the fully developed turbulence region ( $x/L=0.04$ ), predictions of mean velocities using these three models agreed well with experimental data. However, as shown in Figure 4, their performances in the laminar boundary layer region ( $x/L=0.83$ ) were not good as LES models (Figure 2(a)).

## 4. Conclusion

Relaminarization of initially turbulent boundary layer was simulated with large eddy simulation (LES) with the dynamic subgrid scale model. Excellent agreement between prediction and measurement was achieved for mean velocities in turbulent, transitional and laminar boundary layer regions. Good correspondence with experiment was obtained by LES prediction of turbulent intensities. Furthermore, LES reproduced most features of relaminarization process, such as increase of viscous boundary sub-layer thickness and decreasing of turbulent intensity. Predictions of mean velocities with three RANS turbulence models were compared to measured data and it was found their performances in the laminar region were not satisfactory. The results presented in this paper indicate that LES with the dynamic model is capable of modeling the relaminarization, and is recommended in the study of complex flows where laminar, transitional and turbulent flows may coexist.

## References

- [1] Ahmed, S.A. and D.P. Giddens, *Velocity measurement in steady flow through axisymmetric stenoses at moderate Reynolds number*. J. Biomech, 1983. 16: p. 505–516.
- [2] Aupoix, B. and S. Viala, *Prediction of boundary layer relaminarization using low Reynolds number turbulence models*. AIAA Paper, 1995. 95: p. 0862-0876.
- [3] Beech-Brandt, J.J., W.J. Easson, and P.R. Hoskins, *Large eddy simulation of flow in a tube with an axisymmetric stenosis*. ACTA press, 2005. p. 145-150.
- [4] Beratlis, N. E. Balaras, and B. Parvinian, *A numerical and experimental investigation of transitional pulsatile flow in a stenosed channel*. J. Biomech Eng, 2005. 127: p. 1147-1157.
- [5] Corey, B. O. Flint, and C. Robert, *Experimental investigation of turbulent boundary layer relaminarization with application to high-lift systems: preliminary results*. AIAA, 2000. p. 4017-4028.
- [6] Durbin, P. *Near-wall turbulence closure modelling without “damping functions”*. Theoretical and Computational Fluid Dynamics, 1995. 3: p. 1–13.
- [7] Finlay, W.H., K.W. Stapleton, and J. Yokota, *On the use of computational fluid dynamics for simulating flow and particle deposition in the human respiratory tract*. J Aerosol Med, 1996. 9: p. 329–341.
- [8] Germano, M., U. Piomelli, P. Moin, and W. Cabot, *A dynamic subgrid-scale eddy-viscosity model*. Phys. Fluids A, 1991. 3(7): p. 1760-1765.
- [9] Ghalichi, F. X., Y. A. Deng, Y. Douville, M. King, and R. Guidoin, *Low Reynolds number turbulence modeling of blood flow in arterial stenoses*. Biorheology, 1998. 35: p. 281–294.

- [10] Kebede, W. E., B. Launder, and B. A. Younis, *Large amplitude periodic pipe flow: a second-moment closure study*. *Proc. 5<sup>th</sup> Symposium on Turbulent Shear Flows*, 1985. 16: p. 23–29.
- [11] Khalifa, A. M. A. and D. P. Giddens, *Characterization and evolution of post-stenotic flow disturbances*. *J. Biomech*, 1981. 14: p. 279–296.
- [12] Kim, W.W. and S. Menon, *Application of the localized dynamic subgrid-scale model to turbulent wall-bounded flows*. AIAA-97-0210, American Institute of Aeronautics and Astronautics, 35<sup>th</sup> Aerospace Sciences Meeting, Reno, NV, January 1997.
- [13] Launder, B. E. and B. I. Sharma, *Application of the energy-dissipation model of turbulence to the calculation of flow near a spinning disc*. *Letters in Heat and Mass Transfer*, 1974. 1: p. 131-138.
- [14] Launder, B. E., *Laminarization of the turbulent boundary layer by acceleration*. Technical Report 77, MIT Gas Turbine. Lab, 1964.
- [15] Lieber, B. B. and D. P. Giddens, *Post-stenotic core flow behavior in pulsatile flow and its effects on wall shear stress*. *J. Biomech*, 1974. 23: p. 597–605.
- [16] Lien, F. S., G. Kalitzin, and P. A. Durbin, *RANS modeling for compressible and transitional flows*. *Proceedings of Summer Programme, CTR, Stanford University*, 1998. California, USA.
- [17] Lilly, D.K., *A proposed modification of the Germano subgrid-scale closure model*. *Physics of Fluids*, 1992. 4: p. 633-635.
- [18] Luo, X. Y., J. S. Hinton, T. T. Liew, and K. K. Tan, *LES modeling of flow in a simple airway model*. *Medical Engineering&Physics*, 2004. 26: p. 403–413.
- [19] Mittal, R., S. P. Simmons, and F. Najjar, *Numerical study of pulsative flow in a constricted channel*. *J. Fluid Mech*, 2003. 485: p. 337–378.
- [20] Mittal, R., S. P. Simmons, and H.S. Udaykumar, *Application of large-eddy simulation to the study of pulsative flow in a modeled arterial stenosis*. *J. Biomech. Eng*, 2001. 123: p.325–332.
- [21] Moin, P. and K. Mahesh, *Direct numerical simulation: a tool in turbulence research*. *Annu. Rev. Fluid Mech*, 1998. 30: p. 539–578.
- [22] Narasimha, R. and K. R. Sreenivasan, *Relaminarization of fluid flows*. *Adv. Appl. Mech*, 1979. 19: p. 221-269.
- [23] Parsheh, M., A. A. Dahlkild, and P.H. Alfredsson, *Relaminarisation of a turbulent boundary layer in a two-dimensional contraction*. Doctoral Thesis TRITA-MEK 2000. vol 16 (Stockholm, Sweden: KTH).
- [24] Patel, V. C., W. Rodi, and G. Scheuerer, *Turbulence models for near-wall and low Reynolds number flows: a review*. AIAA, 1985. 23: p. 1308–1319.
- [25] Rogallo, R. S. and P. Moin, *Numerical simulation of turbulent flows*. *Annu. Rev. Fluid Mech*, 1984. 16: p.99–137.
- [26] Ryval, J. A., G. Straatman, and D. A. Steinman, *Two-equation turbulence modelling of pulsatile flow in a stenosed tube*. *Journal of Biomechanical Engineering*, 2004. 126: p. 625–635.
- [27] Saad, A. A. and D. P. Giddens, *Flow disturbances through a constricted tube at moderate reynolds numbers*. *Journal of Biomechanics*, 1983. 16: p. 955–963.
- [28] Schlichting, H., *Boundary Layer Theory*. 7<sup>th</sup> edition, McGraw-Hill, 1979.
- [29] Sherwin, S. J. and H. M. Blackburn, *Three-dimensional instabilities and transition of steady and pulsatile axisymmetric stenotic flows*. *Journal of Fluid Mechanics*, 2005. 533: p.297–327.
- [30] Smagorinsky, J., *General circulation experiments with the primitive equations, I. The basic experiment*. *Monthly Weather Review*, 1963. 91: p. 99–164.



- [31] Stroud, J. S., S. A. Berger, and D. Saloner, *Numerical analysis of flow through a severely stenotic carotid artery bifurcation*. Journal of Biomechanical Engineering, 2002. 124: p. 9–20.
- [32] Talamelli, A. N., J. Fornaciari, and H. Westin, *Experimental investigation of streaky structures relaminarizing boundary layers*. Journal of Turbulence, 2002. 3: p. 1-13.
- [33] Varghese, S.V. and S. H. Frankel, *Numerical modeling of pulsatile turbulent flow in stenotic vessels*. Journal of Biomechanical Engineering, 2003. 125: p. 445–460.
- [34] Wilcox, D.C., *Reassessment of the scale determining equation for advanced turbulence models*. AIAA, 1988. 26: p. 1299-1306.
- [35] Zhang, Z. and C. Kleinstreuer, *Low-Reynolds-number turbulent flows in locally constricted conduits: a comparison study*. AIAA, 2003. 41: p. 831–840.
- [36] Wang, M. and Q. Chen, *Assessment of various turbulence models for flows in enclosed environment (rp-1271)*. HVAC&R Research, 2009. 15(6): p. 1099–119.
- [37] Kim, S. E., *Large eddy simulation using an unstructured mesh based finite-volume solver*. Proc 34<sup>th</sup> AIAA Fluid Dynamics Conference and Exhibit, AIAA 2004–2548: p. 1–17. 2004. Portland, Oregon, USA.